

ADME-Guided Design and Synthesis of Aryloxanyl Pyrazolone Derivatives To Block Mutant Superoxide Dismutase 1 (SOD1) Cytotoxicity and Protein Aggregation: Potential Application for the Treatment of Amyotrophic Lateral Sclerosis

Tian Chen,[†] Radhia Benmohamed,[‡] Jinho Kim,^{§,||} Karen Smith,[⊥] Daniel Amante,^{§,||} Richard I. Morimoto,[#] Donald R. Kirsch,[‡] Robert J. Ferrante,^{§,||} and Richard B. Silverman^{*,†,∞}

[†]Department of Chemistry, Northwestern University, Evanston, Illinois 60208-3113, United States

[‡]Cambria Pharmaceuticals, Cambridge, Massachusetts, 02142, United States

[§]Departments of Neurological Surgery, Neurology, and Neurobiology, University of Pittsburgh, Pittsburgh, Pennsylvania 15213, United States

^{||}Geriatric Research Educational and Clinical Center (00-GR-H), V.A. Pittsburgh Healthcare System, 7180 Highland Drive, Pittsburgh, Pennsylvania 15206, United States

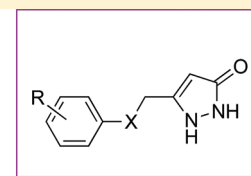
[⊥]Bedford VA Medical Center, 200 Springs Road, Bedford, Massachusetts 01730, United States

[#]Department of Molecular Biosciences, Rice Institute for Biomedical Research, Northwestern University, Evanston, Illinois 60208-3500, United States

[∞]Department of Molecular Biosciences, Chemistry of Life Processes Institute, Center for Molecular Innovation and Drug Discovery, Northwestern University, Evanston, Illinois 60208-3113, United States

Supporting Information

ABSTRACT: Amyotrophic lateral sclerosis (ALS) is an orphan neurodegenerative disease currently without a cure. The arylsulfanyl pyrazolone (ASP) scaffold was one of the active scaffolds identified in a cell-based high throughput screening assay targeting mutant Cu/Zn superoxide dismutase 1 (SOD1) induced toxicity and aggregation as a marker for ALS. The initial ASP hit compounds were potent and had favorable ADME properties but had poor microsomal and plasma stability. Here, we identify the microsomal metabolite and describe synthesized analogues of these ASP compounds to address the rapid metabolism. Both in vitro potency and pharmacological properties of the ASP scaffold have been dramatically improved via chemical modification to the corresponding sulfone and ether derivatives. One of the ether analogues (**13**), with superior potency and in vitro pharmacokinetic properties, was tested in vivo for its pharmacokinetic profile, brain penetration, and efficacy in an ALS mouse model. The analogue showed sustained blood and brain levels in vivo and significant activity in the mouse model of ALS, thus validating the new aryloxanyl pyrazolone scaffold as an important novel therapeutic lead for the treatment of this neurodegenerative disorder.



X = SO, SO₂, O
 R = alkyl, aromatic and/or halogen groups

INTRODUCTION

Amyotrophic lateral sclerosis (ALS), also known as Lou Gehrig's disease, is a fatal neurodegenerative disease resulting in progressive muscle loss and paralysis.¹ The incidence of ALS is 1–2 per 100 000 per year,^{2,3} with approximately 2–5 years from diagnosis to death. There is a disproportionate incidence of ALS among military personnel, particularly among Gulf War veterans.^{4–6} No effective treatment for the disease is currently known.⁷ Riluzole, the only FDA approved drug for treating ALS, extends patient lives by 2–3 months.⁸

The sporadic disease (SALS) accounts for approximately 90% of all cases and familial disease (FALS) the remaining 10%. Over 100 mutations in Cu/Zn superoxide dismutase 1 (SOD1) have been identified since the pioneering work of Brown and colleagues in identifying this FALS gene,⁹ and studies on SOD1

have advanced the understanding of the molecular mechanisms and underlying pathogenesis of this disease.¹⁰ Mutations in SOD1 are believed to be responsible for about 20% of all FALS cases.^{11,12} The latter findings resulted in the development of transgenic mouse models, which have further elucidated pathophysiological mechanisms as well as provided a model for preclinical drug trials.¹³ The clinical and pathological features of FALS and sporadic ALS are similar, which supports the strategy of using laboratory models of FALS mutations for elucidating disease pathogenesis and for identifying potential therapeutic targets for both forms of the disease.^{14,15} Protein aggregation is a pathological hallmark of ALS;^{13,16} the

Received: October 21, 2011

Published: December 22, 2011

appearance of intracellular inclusions containing detergent-insoluble SOD1 protein aggregates represents a common early event associated with SOD1 cellular toxicity.^{17,1}

In previous studies, PC12 cells expressing mutant G93A SOD1 were utilized in a cell-based high throughput screening (HTS) assay.^{18,19} The arylsulfanyl pyrazolone (ASP) scaffold was identified as one of the active scaffolds showing protection against cytotoxicity from protein aggregation from a 50 000-compound library screened in the HTS assay (Figure 1; two

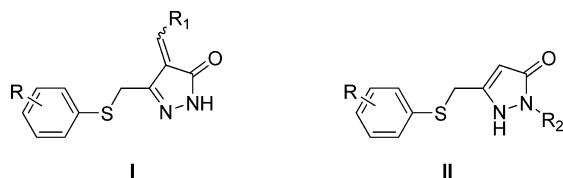
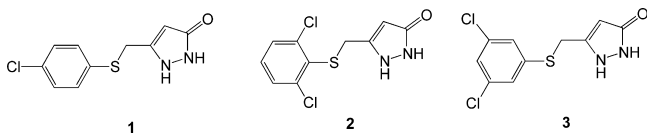


Figure 1. ASP HTS hits: R₁, alkyl or substituted aromatic groups; R₂, proton or substituted aromatic groups; R, various alkyl and/or halogen groups.

general structures were active, where type II was, in general, more potent than type I).²⁰ Structural optimization of this scaffold led via **1** (EC₅₀ = 1.93 μM) and **2** (EC₅₀ = 0.71 μM) to a more potent analogue (**3**) than the original screening hits, with an EC₅₀ of 170 nM. In vitro pharmacokinetic (PK) and in vivo brain/plasma ratio studies were also performed at an early stage of this drug development project. Other than having low microsomal stability and plasma stability, the ASP scaffold generally showed good PK properties and permeated the blood–brain barrier.²¹ Identifying and modifying the metabolic liability in the ASP scaffold, therefore, became a priority. The results of the metabolism studies, SAR investigations of the new scaffold, PK and toxicity properties, the ability to cross the blood–brain barrier, and effects on an ALS mouse model are described herein.



RESULTS AND DISCUSSION

Chemistry. ASP analogues were synthesized as described earlier.²¹ The syntheses of type II ASP analogues with sulfoxide and sulfone linkers in place of the sulfide are shown in Scheme 1. The sulfide linker β-ketoester intermediates (**20–22**) were treated with VO(acac)₂-TBHP^{22,23} to give the sulfoxide and sulfone intermediates (**23–26**) or with H₂O₂²⁴ to give sulfone **27**, which were treated with hydrazine to give the corresponding sulfoxide (**4, 5**) and sulfone (**6–8**) products. The corresponding type II aryloxanyl pyrazolone derivatives (**9–14**) were prepared from phenol and ethyl 4-chloroacetoacetate to generate the β-hydroxyester intermediates (**28–33**),²⁵ followed by treatment with hydrazine (Scheme 2). Although this two-step synthetic method is simple and direct, it is not efficient mainly because of the low stability of the enolate derivatives from both the ethyl 4-chloroacetoacetate and the β-hydroxyester intermediates. Improved strategies to prepare the β-hydroxyester intermediates are described in Scheme 3. Compounds **42–47** were synthesized from the corresponding phenols and 2-bromo-*N*-methoxy-*N*-methylacetamide, which

was obtained from 2-bromoacetyl bromide and *N,O*-dimethylhydroxylamine hydrochloride.²⁶ The corresponding β-hydroxyester intermediates were prepared by condensation of **42–47** with the enolate of ethyl acetate. The aryloxanyl pyrazolones (**13–19**) were obtained by treatment of the β-hydroxyester intermediates with hydrazine. Intermediates **39** and **41** were obtained via Suzuki coupling of aryl bromides **38** and **40**, respectively, with phenylboronic acid using a palladium catalyst.²⁷

To avoid hydrolysis of Weinreb amide **36** under concentrated and strong basic conditions,^{28,29} 3,5-dichlorophenol (**34**) was allowed to react with ethyl 2-bromoacetate and then treated with NaOH/H₂O to afford **35**. This intermediate was transformed to **42** with oxalyl chloride and *N,O*-dimethylhydroxylamine hydrochloride, and the Weinreb amide was converted to **13** as described above.

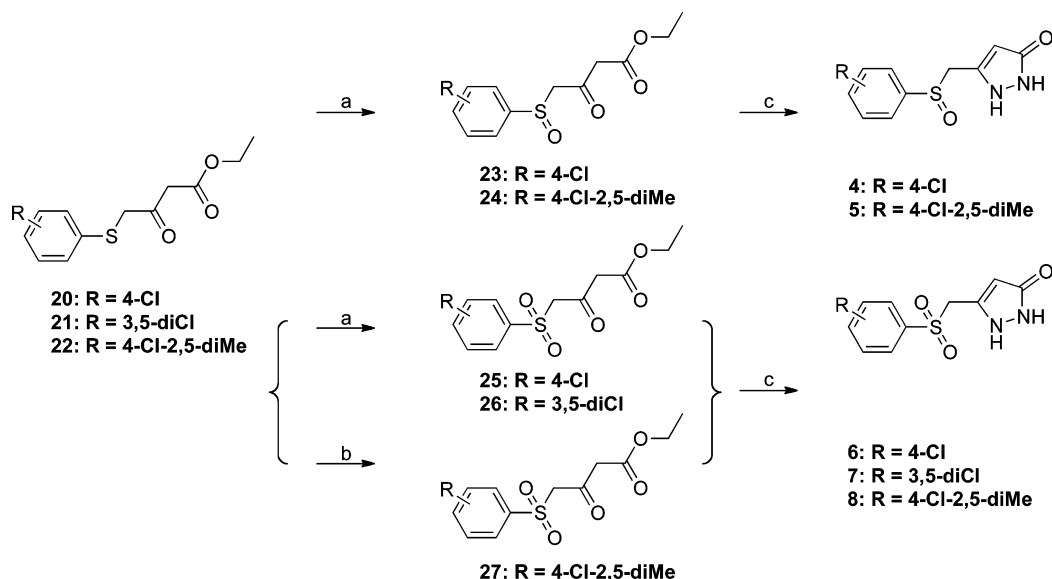
Microsomal Stability. ASP analogues, like 5-((2,4-dichloro-5-methylphenylthio)methyl)-1*H*-pyrazol-3(2*H*)-one (**48**, Figure 2) and 5-((4-chloro-2,5-dimethylphenylthio)methyl)-1*H*-pyrazol-3(2*H*)-one (**49**), were found to have low mouse liver microsomal stability. One possible site of metabolism by cytochrome P450 (CYP) isozymes³⁰ is the aromatic methyl group. Therefore, an analogue lacking an aromatic methyl group (**1**) was tested for microsomal stability in the presence of NADPH, and the results were compared to minaprine (**50**), an antidepressant drug known to undergo rapid microsomal metabolism, as a positive control.³¹ After incubation for 20 min with rat liver microsomes, minaprine and **1** were metabolized by 41% and 88%, respectively (Figure 3). Therefore, the aromatic methyl group is not responsible for the metabolic instability of **1**. On the basis of the above result, the most likely site of CYP metabolism is the sulfide sulfur atom, which is known to undergo oxidative metabolism.³²

Metabolite Profiling of 1. Metabolic profiling was carried out on **1** despite its relatively low in vitro potency and because it contained a chlorine atom, which has a natural isotope abundance (³⁵Cl/³⁷Cl = 3:1) that can simplify the mass spectral analysis. The two likely metabolites are the corresponding sulfoxide (**4**) and sulfone (**6**), which were synthesized as shown in Scheme 1.

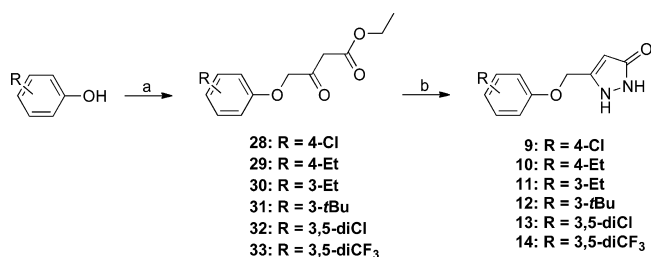
Compound **1** (15 μM) was incubated with rat liver microsomes at 37 °C for 0, 5, 10, 20, and 60 min in the presence of NADPH. HPLC analysis showed a new peak (5.90 min) that was not present prior to the addition of microsomes and that was identified as the corresponding sulfoxide by comparison with those of synthetic standards of sulfoxide **4** (5.95 min) and sulfone **6** (10.8 min) (Figure 4).

Because of the limit of HPLC detection, the metabolite profiling of **1** was also carried out by LC/MS/MS. To assist in this analysis, an analogue of **1** with ¹⁵N substituted for both pyrazole nitrogens was synthesized by the route in Scheme 1 using ¹⁵NH₂–¹⁵NH₂ in place of hydrazine. Both **1** and [¹⁵N₂]**1** (5 μM) were incubated with rat liver microsomes in the presence and absence of NADPH. After 0, 10, 20, 40, and 60 min, the samples were processed and analyzed by LC/MS/MS. Both compounds, in the presence of NADPH but not in its absence, produced one new peak not detected in the controls without microsomes or compound. The mass spectrum of the new peak corresponded to the sulfoxide (**4**). No sulfone was detected. The rate of formation of sulfoxide corresponded well with the loss of the sulfide (Figure 5).

Metabolism Guided Design and Synthesis of ASP Analogues. Because of the rapid metabolism of **1**, the sulfide

Scheme 1^a

^aReagents and conditions: (a) TBHP, VO(acac)₂, DCM, room temperature, overnight; (b) H₂O₂, AcOH, EtOAc, room temperature; (c) NH₂NH₂, EtOH, room temperature, overnight.

Scheme 2^a

^aReagents and conditions: (a) ethyl 4-chloroacetoacetate, NaH, THF, DMF, -20 to 70 °C; (b) NH₂NH₂, EtOH, room temperature, overnight.

was replaced by sulfoxide, sulfone, and ether functional groups, synthesized as shown in Schemes 1–3. These compounds were screened in the toxicity protection assay, and compounds that retained activity in this assay were tested for in vitro microsomal stability.

Mutant SOD1-Induced Cytotoxicity Protection Assay of Modified Compounds. All of the ASP analogues exhibited 100% viability in the cytotoxicity protection assay except for **4** (maximum viability of ~35%). The EC₅₀ values of these analogues in the protection assay are summarized in Table 1. In general, the potencies of the analogues were greater with the ether linkage when compared with the sulfide, sulfone, and sulfoxide. The low sulfoxide potency indicated that metabolism of the ASPs to the corresponding sulfoxide results in deactivation of the compounds and that pursuing a prodrug strategy with the thioether linked compounds would not be possible. Therefore, a series of ether analogues, aryloxanyl pyrazolones, was synthesized (Table 1). Ether **13** (CMB-087229) was the most potent (67 nM) of these compounds. Analogues of **13**, having F, CF₃, Br, and Ph in place of the Cl atoms, indicated that size and electronics were important features at the meta-positions; the potency decreased in the following order: Cl > CF₃ > F > Br > Ph.

In Vitro ADME Assays. Microsomal Stability. Human and mouse microsomal stabilities of sulfone **7** and ether analogues **9** and **13** were tested at 5 μM at 37 °C for 1 h in the presence and absence of NADPH (Table 2). All three compounds showed good stability.

Aqueous Solubility. The aqueous solubility of **7**, **9**, and **13** was evaluated by diluting them from a stock solution in DMSO to a final concentration of 1% DMSO in PBS (Table 3). The maximum solubility was considered to be the highest concentration that showed no precipitation. All three compounds showed good aqueous solubility.

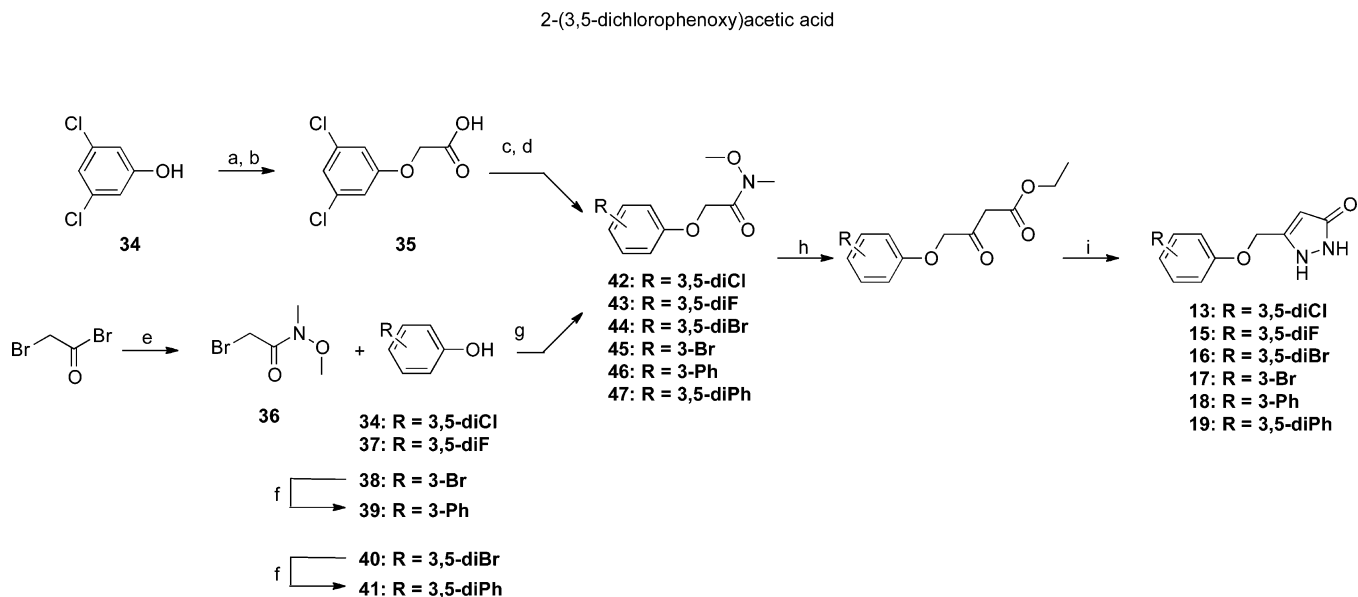
Caco-2 Permeability. Compounds **7**, **9**, and **13** all had high³³ permeability in the Caco-2 permeability assay (Table 4).

Protection of Primary Cortical Neurons. It is not uncommon to observe that compounds that are active in tissue culture cells will not be active in differentiated neurons. Therefore, sulfide **2**, sulfone **7**, and ether linker analogue **13** were tested in a primary cortical neuron cell protection assay that showed that all of these compounds were active. This issue was of particular concern because compounds from another scaffold, cyclohexane 1,3-diones, identified in the original high-throughput screen had poor activity in this assay, potentially due to poor cell permeability.³⁴

PK Profiling of **13.** Sulfone **7** and ether linker analogues **9** and **13** all showed good or adequate in vitro ADME properties. Compound **13** was selected based on its potency and in vitro pharmacological profile for in vivo PK profiling and efficacy in a mouse model of ALS.

Mouse in Vivo Steady-State Level and Blood–Brain Barrier Penetration for **13.** The in vivo steady-state level of ether analogue **13** from plasma was determined in mice. The animals were administered 300 mg/kg **13** and sacrificed at progressive time points (0, 3, 6, 12, and 24 h, Table 5). Blood and brain samples were harvested and analyzed by mass spectrometry using ESI ionization in the MRM mode.

In Vivo Rat PK Profiling of **13.** Compound **13** was administered to Sprague–Dawley rats both intravenously and

Scheme 3^a

^aReagents and conditions: (a) ethyl 2-bromoacetate, NaOEt, EtOH, reflux, overnight; (b) NaOH, H₂O, 80 °C, overnight; (c) oxalyl chloride, DCM, DMF, room temperature, 4 h; (d) *N,O*-dimethylhydroxylamine hydrochloride, DIEA, DCM, room temperature, 1 h; (e) *N,O*-dimethylhydroxylamine hydrochloride, K₂CO₃, Et₂O, H₂O, room temperature, 30 min; (f) phenylboronic acid, PdCl₂(PPh₃)₂, K₂CO₃, dioxane, H₂O, 100 °C, 16 h; (g) NaOEt, EtOH, 70 °C, overnight; (h) EtOAc, LiHMDS, THF, -78 °C, overnight; (i) NH₂NH₂, EtOH, room temperature, overnight.

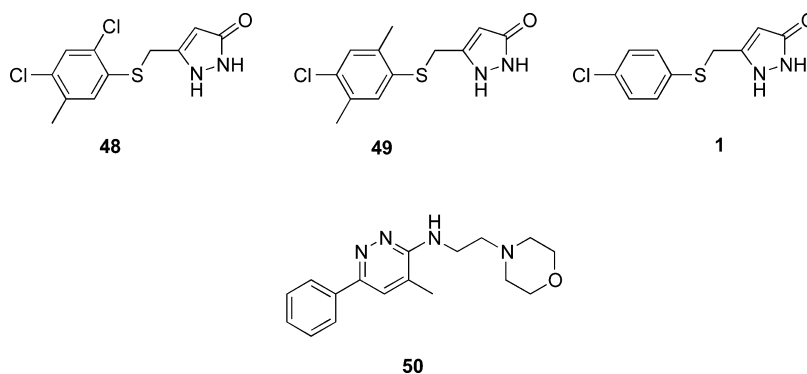


Figure 2. Compounds tested in metabolic studies.

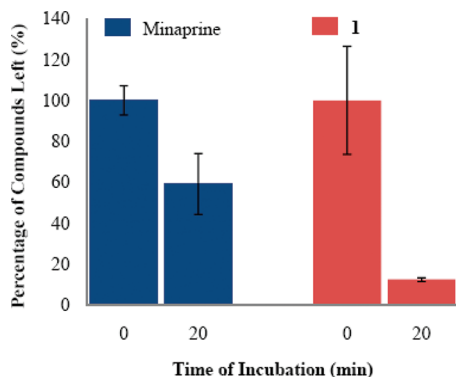


Figure 3. Microsomal stability of minaprine (50) and 1. Rat liver microsomes were incubated at 37 °C for 20 min in the presence of 15 μM compound.

orally at 1 mg/kg in a single bolus dose. The results are summarized in Table 6.

Effect of 13 on the Potassium Channel. The *in vitro* effect of 13 (10 μM) on the hERG potassium channel current

expressed in human embryonic kidney cells (HEK293) was evaluated using a patch-clamp technique, the most definitive *in vitro* hERG inhibition assay.³⁵ A positive control (E-4031) was used to confirm the sensitivity of this test system, and the TurboSol evaluation system was performed on 13 to confirm that its insolubility was not a reason for low hERG inhibition observed in this test system (see Supporting Information for results). The mean percent hERG antagonism (two experiments) was 0.6 ± 1.5%. These results indicate that 13 does not affect the hERG channel.

Effect of 13 on Cytochrome P450 Isozymes. Compound 13 was tested for its inhibition of CYP1A2, CYP2C9, CYP2C19, CYP2D6, and CYP3A4, present in human liver microsomes. IC₅₀ values of 13 to CYP isozymes inhibition were evaluated using single drug substrates except for CYP3A4 (testosterone and midazolam tested). IC₅₀ values were >50 μM except for CYP2C19, which was 20 μM.

Effect of 13 on Enzymes and Receptors. Compound 13 was screened at 10 μM in duplicate by MDS Pharma Services (Taipei, Taiwan) with LeadProfilingScreen, a suite of 68 *in vitro* enzyme and receptor assays of the most commonly

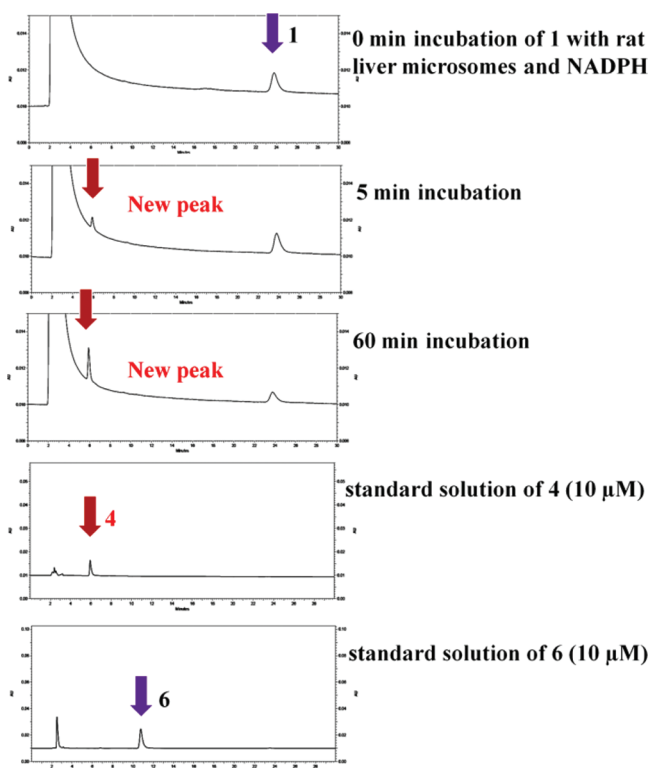


Figure 4. HPLC traces of the incubation of **1** ($15 \mu\text{M}$) with rat liver microsomes at 37°C .

observed adverse CNS, cardiovascular, pulmonary, and genotoxic activities. No significant activity was detected in any of the 68 assays. See Supporting Information for results.

Effect of 13 Administration on SOD1 G93A ALS Mice. Control and transgenic mice of the same age (± 3 days) and from the same “F” generation were selected from multiple litters to form experimental cohorts. The tolerable dose range for **13** was determined in wild type mice by increasing the dose b.i.d. one-fold each ip injection; the maximum tolerated dose was 75 mg/kg . On the basis of the studies performed to determine tolerance and blood brain levels, the dose levels of 1.0 , 10 , and 20 mg/kg once a day were administered, starting at 6 weeks of age, throughout the lives of the G93A mice. Administration of **13** resulted in a significant extension in survival in the G93A

ALS mice in a dose dependent manner in comparison to untreated G93A mice (Figure 6). The most efficacious dose (20 mg/kg) resulted in a life extension of 13.3% .

DISCUSSION

We had previously found that ASP compounds are metabolically unstable.²⁹ In vitro metabolic studies were carried out to determine the basis of microsomal instability. The early analogues had aromatic methyl groups (**48** and **49**) and a sulfide sulfur atom. Metabolic degradation of an ASP without an aromatic methyl (**1**) was more rapid than that of minaprine (**50**), a CNS drug known to undergo rapid metabolism, indicating that the instability was not caused by the aromatic methyl (Figure 3). Following microsome incubation, a new metabolite of **1** was identified by HPLC (Figure 4), which comigrated with the corresponding sulfoxide (**4**); no sulfone (**6**) was detected. The formation of sulfoxide **4** quantitatively followed the degradation of **1** (Figure 5). The structure of the NADPH-dependent metabolite was further confirmed by LC/MS/MS; the NADPH dependence suggests that metabolism is catalyzed by a cytochrome P450.

Identification of the metabolite of **1** as the corresponding sulfoxide, which had poor activity in the cytotoxicity protection assay, guided our redesign of the arylsulfanyl pyrazolones to the corresponding sulfones and ethers (aryloxanyl pyrazolones). In general, the potency of compounds with the various linker groups increases (EC_{50} decreases) in the order ether > sulfide > sulfone \gg sulfoxide.

A series of ether analogues was synthesized (Table 1), and all of the compounds were assayed in the cytotoxicity protection assay, which uses PC12 cells that express mutant G93A SOD1 as a YFP fusion protein.²⁰ In general, the most potent analogues were the 3,5-disubstituted phenyl analogues, where dichloro > dibromo > ditrifluoromethyl > difluoro > diphenyl. The dichloro analogue (**13**) has an EC_{50} of 67 nM .

Sulfone **7**, ether **9**, and ether **13** were much more metabolically stable than arylsulfanyl pyrazolone **1**,²⁹ with the ether being considerably more stable than the sulfone (Table 2). Because of the stability of the ethers, further ADME testing was carried out with the most potent analogue (**13**).

The aqueous solubility of ether **13** was good ($250 \mu\text{M}$) compared with that of **48** ($56 \mu\text{M}^{21}$), although the solubility of sulfone **7** was greater than twice that of **13**. Permeability through Caco-2 monolayer cells correlates with in vivo

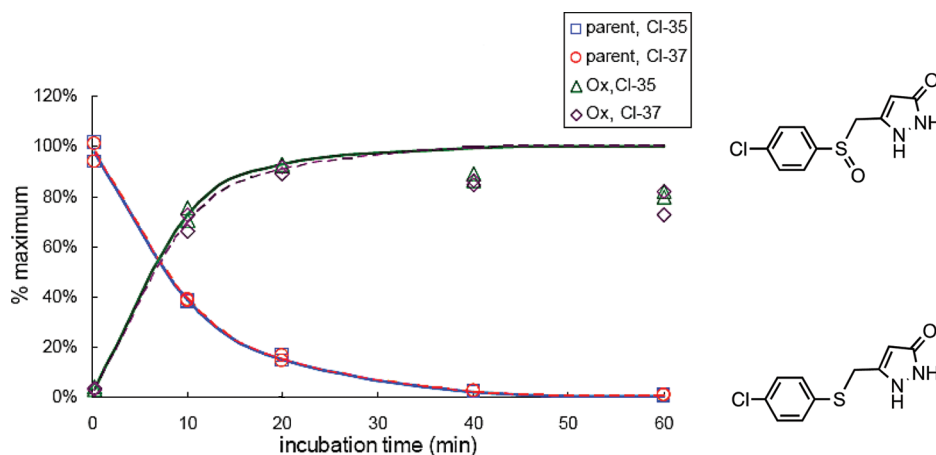
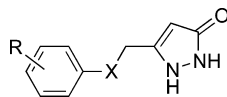


Figure 5. Rate of formation of sulfoxide **4** and rate of metabolism of **1**.

Table 1. SAR of ASP Analogues with -S-, -SO-, -SO₂-, and -O- Linkers^a

X	compd	R	EC ₅₀ (μM)
S	1	4-Cl	1.93
	2	2,6-di-Cl	0.71
	3	3,5-di-Cl	0.17
SO	4	4-Cl	>32
	5	4-Cl-2,5-di-Me	2.88
SO ₂	6	4-Cl	4.7
	7	3,5-di-Cl	1.41
	8	4-Cl-2,5-di-Me	1.47
O	9	4-Cl	0.79
	10	4-Et	1.96
	11	3-Et	0.72
	12	3- <i>t</i> -Bu	0.87
	13	3,5-di-Cl	0.067
	14	3,5-di-CF ₃	0.58
	15	3,5-di-F	1.07
	16	3,5-di-Br	0.51
	17	3-Br	1.02
	18	3-Ph	2.84
	19	3,5-di-Ph	3.70

^aAverage *Z'* factor is 0.5.

Table 2. In Vitro Microsomal Stability of 7, 9, and 13^c

compd	human			mouse		
	CL' _{int} ^a (mL min ⁻¹ kg ⁻¹)	T _{1/2} ^b (min)	CL' _{int} NADPH-free (mL min ⁻¹ kg ⁻¹)	CL' _{int} ^a (mL min ⁻¹ kg ⁻¹)	T _{1/2} ^b (min)	CL' _{int} NADPH-free (mL min ⁻¹ kg ⁻¹)
7	4.5	>60	1.3	15.3	>60	0
9	15.3	139	0	24.5	143	6.1
13	25	93	13	64	36	21

^aMicrosomal intrinsic clearance. ^bHalf-life. ^cExperimental procedures and data analysis are described in ref 29. Data were obtained from Aprelica and Biogen Idec.

Table 3. In Vitro Aqueous Solubility of Compounds 7, 9, and 13^a

compd	maximum solubility (μM)	
	45 min	16 h
7	≥500	≥500
9	250	250
13	250	250

^aData were obtained at Aprelica Inc. Experimental procedures and data analysis are described in ref 21.

Table 4. In Vitro Caco-2 Permeability of 7, 9, and 13^a

compd	P _{app} (A→B) ^b (10 ⁻⁶ cm/s)	P _{app} (B→A) ^b (10 ⁻⁶ cm/s)	ratio (B→A)/(A→B)
7	27.0	4.4	0.2
9	43.0	28.0	0.6
13	36.7	14.1	0.4

^aData were obtained from Aprelica Inc. Experimental procedures and data analysis are described in ref 21. ^bApparent permeability.

intestinal permeability. The efflux of compounds in the opposite direction also can be estimated by this method. The high permeability values (P_{app} = 27–43 × 10⁻⁶ cm/s) and low efflux ratios (P_{app}(B→A)/P_{app}(A→B) of 0.2–0.6) of 7, 9, and

Table 5. In Vivo Plasma Concentration of Compound 13^a

time (h)	plasma concn (μg/mL [μM])
0	0
3	88.8 [342]
6	90 [347]
12	64.4 [248]
24	1.7 [6.5]

^aBrain and plasma samples were analyzed at Aprelica, Inc.

13 suggest that these compounds have high membrane permeability³⁶ and are likely poor substrates for efflux transport proteins, such as P-glycoprotein.³⁷

To determine if these compounds are active in other types of cells, including neurons, a screen of selected compounds was carried out with four other cell types: SHSY-5Y, HeLa, HEK293, and primary cortical neuronal cells. Ether 13 was active in all four cell types, which is a positive indication of utility for the treatment of ALS, a non cell autonomous disease.³⁸

Compound 13 was evaluated for its metabolic stability and blood–brain barrier penetration in mice. Mouse plasma stability was good, peaking at 3–6 h; after 4 h 13 was detected at 194 μM in brain tissue. The loss of 13 does not follow first-order kinetics following intraperitoneal administration. Phar-

Table 6. Rat Plasma PK Profile of Compound 13^a

	AUC last (ng h/mL)	AUC/dose (ng h mL ⁻¹ dose ⁻¹)	T _{1/2} (h)	CL (mL min ⁻¹ kg ⁻¹)	V _{ss} (L/kg)	C _{max} (ng/mL)	T _{max} (h)	F (%)
iv	179	184	2.1	92	5.7			
po	42	50	3.6			39	0.25	27

^aSingle bolus administration of 1 mg/kg iv and po to SD rats. Data were obtained from Biogen Idec.

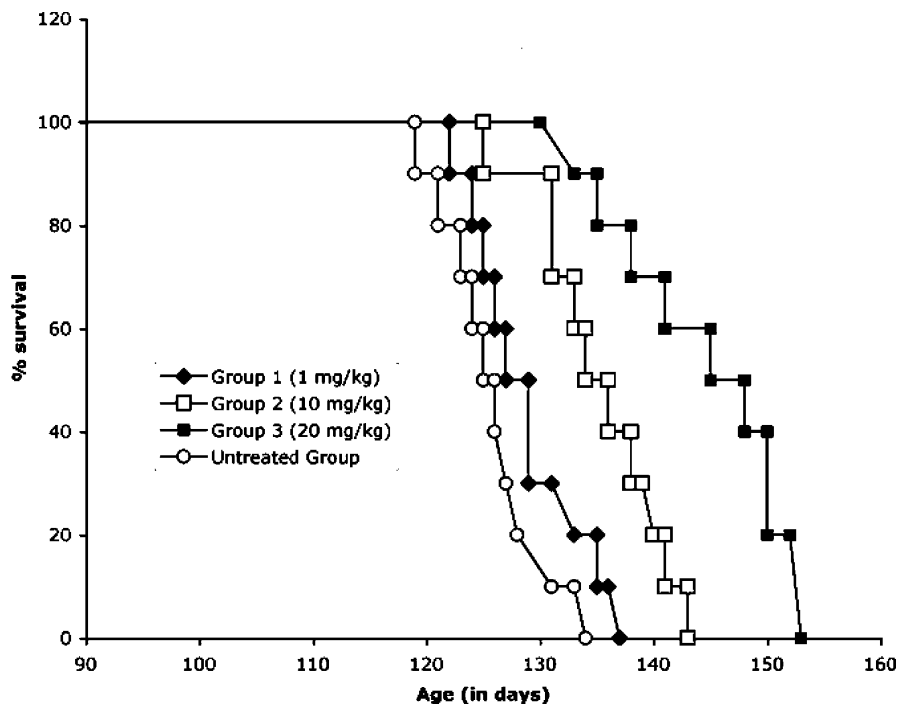


Figure 6. Kaplan–Meier plot of 13-treated SOD1 G93A ALS mice: untreated group, 125.7 ± 4.9 days; group 1 (1 mg/kg), 129.2 ± 5.3 days; group 2 (10 mg/kg), 135 ± 5.5 days; group 3 (20 mg/kg), 142.5 ± 8.2 days; $p < 0.05$.

macokinetics could be influenced by the high plasma protein binding by 13 (98% in rat and human), which can limit compound bioavailability in the plasma compartment, thereby prolonging the half-life.^{39,40} However, high plasma protein binding alone does not determine the effect on the pharmacokinetic properties; the binding affinity (on/off rate) also is a major factor. Pharmacokinetics in Sprague–Dawley rats was investigated both by iv and po administration. The compound appears to be reasonably stable and is orally active; half-lives were 2.1 and 3.6 h, respectively, for these two routes of administration with oral bioavailability (F) of 27%, which is above the typical cutoff for continued development of drug candidates⁴¹ (Table 6). The difference in plasma stability from the mouse and rat studies could be the result of a combination of factors, including different species (mouse vs rat), different amount of compound used (5 mg/kg vs 1 mg/kg), and route of administration (ip vs iv).

Toxicity is an important cause for attrition of drug candidates at later stages of drug development. To reduce the time and effort of drug discovery, various toxicological criteria need to be met early in the development of drug candidates. One is the effect of the compound on the human ether-a-go-go-related gene (hERG), a gene that encodes a cardiac potassium ion channel to regulate cardiac repolarization, which determines cardiac rhythmicity. When a compound inhibits the hERG ion channel, it can produce a disorder called long QT syndrome, resulting in torsade de pointes, heart arrhythmias and potentially sudden death. Therefore, it is essential that drug

candidates do not affect hERG. Compound 13 did not antagonize hERG at 10 μ M.

Cytochrome P450 isozymes are also associated with drug toxicity.⁴² Molecules that either inhibit or up-regulate these enzymes can cause drug–drug interactions. If they inhibit the isozymes, metabolism of other drugs is blocked. If they up-regulate the isozymes, it leads to rapid metabolism of drugs. The IC₅₀ of compound 13 was >50 μ M for human liver CYP1A2, CYP2C19, CYP2D6, and CYP3A4 and was 20 μ M for CYP2C9, indicating that 13 should not cause drug–drug interactions.

To determine if there are other receptors or enzymes that might be potential off-targets, 13 was screened by MDS Pharma Services (Taipei, Taiwan) using its LeadProfilingScreen, a suite of 68 in vitro enzyme and receptor assays of the most commonly observed adverse CNS, cardiovascular, pulmonary, and genotoxic activities. Compound 13 showed no significant binding to any of these targets at 10 μ M, suggesting that it is highly target selective.

Expression of genes with ALS-associated G93A SOD1 mutations produces a striking ALS phenotype motor neuron degeneration and paralysis in rats.^{43,44} Transgenic mice that express human G93A mutant SOD1 develop hind limb weakness, muscle wasting, and neuropathological sequelae similar to those observed in both familial and sporadic ALS patients.⁴⁵ Candidate compounds are commonly tested in the ALS mouse model to evaluate their potential for the treatment of ALS.¹³ The in vivo efficacy of riluzole, the only FDA-

approved drug for ALS, was tested in G93A SOD1 mice and showed a lifespan extension of 7.5% when tested at 16 mg/kg⁴⁶ and of 11% at 22 mg/kg.⁴⁷ The in vivo efficacy of **13** in the mutant SOD1 G93A ALS mouse model was assessed to validate the aryloxanyl pyrazolone scaffold as a potential therapy for ALS. Compound **13** produced a life extension of 13.3% at 20 mg/kg (Figure 6), comparable to or superior to riluzole.

CONCLUSIONS

We had previously identified arylsulfanyl pyrazolones (ASP) as a class of compounds exhibiting good potency against toxicity from protein aggregation by mutant SOD1.²¹ These compounds could not be developed further, however, because of poor metabolic stability. Here we identify the cause for metabolic instability as the sulfide sulfur atom, which is oxygenated to the corresponding sulfoxide and show that the resulting sulfoxide compounds have significantly lower activity than the sulfides. Conversion to the corresponding sulfones and ethers, the aryloxanyl pyrazolones, resulted in much greater metabolic stability. The most potent analogue was aryloxanyl pyrazolone **13**, with an IC₅₀ of 67 nM, having good aqueous solubility, excellent Caco-2 permeability with low efflux potential, a rat plasma half-life of 3.6 h, rat oral bioavailability of 27%, neuron permeability, good mouse blood–brain barrier penetration (194 μM after 4 h), no effect on the hERG channel or 68 off-target proteins, and a life extension of G93A ALS mice of 13.3% at 20 mg/kg, as good or better than that previously reported for riluzole, the only FDA-approved therapeutic for ALS. These results support **13** as a novel drug candidate for the treatment of ALS.

EXPERIMENTAL SECTION

Chemistry. General Methods, Reagents, and Materials. All reagents were purchased from Aldrich Chemical Co. (Milwaukee, WI) or Alfa Aesar (Ward Hill, MA) and were used without further purification, unless stated otherwise. Tetrahydrofuran was distilled under nitrogen from sodium/benzophenone. Dichloromethane was redistilled from CaH₂ under nitrogen. Other dry solvents were directly purchased. Thin-layer chromatography was carried out on E. Merck precoated silica gel 60 F₂₅₄ plates. Compounds were visualized with ferric chloride reagent or a UV lamp. Column chromatography was performed with E. Merck silica gel 60 (230–400 mesh). Proton nuclear magnetic resonances (¹H NMR) were recorded in deuterated solvents on a Varian Inova 400 (400 MHz), a Varian Inova 500 (500 MHz), or a Bruker 500 (500 MHz) spectrometer. Chemical shifts are reported in parts per million (ppm, δ) using various solvents as internal standards (CDCl₃, δ 7.26 ppm; DMSO-*d*₆, δ 2.50 ppm). ¹H NMR splitting patterns are designated as singlet (s), doublet (d), triplet (t), or quartet (q). Splitting patterns that could not be interpreted or easily visualized were recorded as multiplet (m) or broad (br). Coupling constants are reported in hertz (Hz). Proton-decoupled carbon (¹³C NMR) spectra were recorded on a Varian Inova 500, a Varian Inova 400, or a Bruker 500 (125.7, 100.6, and 125.7 MHz, respectively) spectrometer and are reported in ppm using various solvents as internal standards (CDCl₃, δ 77.23 ppm; DMSO-*d*₆, δ 39.52 ppm). Electrospray mass spectra were obtained using an LCQ-Advantage spectrometer with methanol as the solvent in the positive ion mode. High-resolution mass spectrometry was carried out using a VG70-250SE mass spectrometer. Chemical ionization (CI) or electron impact (EI) was used as the ion source. Elemental analyses were performed by Atlantic Microlab Inc., Norcross, GA. All final compounds were analyzed for purity by HPLC using a Luna C18 (2) column (4.6 mm × 150 mm, 5 μm; Phenomenex, Torrance, CA) at a flow rate of 1 mL/min with multiple HPLC conditions. Sample elution was detected by absorbance at 254 nm. HPLC was performed on a

Beckman System Gold chromatograph (model 125P solvent module and model 166 detector). All tested compounds had a purity of at least 95% as demonstrated by HPLC (see Supporting Information).

5-(4-Chlorophenylthio)-1H-[¹⁵N₂]pyrazol-3(2H)-one (3). 4-Chlorothiophenol (1.1 g, 7.61 mmol) was mixed with ethyl 4-chloroacetoacetate (0.95 mL, 7.00 mmol) in CH₂Cl₂ (100 mL) at 0 °C. Triethylamine (1.5 mL, 10.8 mmol) was then added dropwise. After the resulting suspension was stirred at 0 °C for another 30 min, the reaction mixture was poured into water, and the aqueous layer was extracted with EtOAc. The combined organic layer was washed with saturated NaHCO₃, HCl (0.25 N), brine, concentrated in vacuo, and purified by flash column chromatography (ethyl acetate/hexanes = 1/9) to afford **20** (1.82 g) as a light yellow oil, which was not very stable. Therefore, **20** was used directly in the next step immediately after flash column chromatography purification. A proton NMR spectrum was taken immediately after the flash column purification. ¹H NMR (400 MHz, CDCl₃, δ): 7.37 (dd, *J* = 18.4, 8.4 Hz, 4H), 4.12 (d, *J* = 14.0, 7.2 Hz, 2H), 4.06 (s, 2H), 3.72 (s, 2H), 1.21 (t, *J* = 7.2 Hz, 3H). Compound **20** (0.52 g, 1.89 mmol) was stirred in EtOH (15 mL) and H₂O (6 mL), then ¹⁵NH₂¹⁵NH₂·H₂SO₄ (0.25 g, 1.89 mmol) and NaHCO₃ (0.32, 3.79 mmol) were added. The resulting solution was stirred overnight at room temperature, during which time a precipitate formed. The precipitate was filtered, washed with cold EtOH, and dried in vacuo to afford **3** (0.21 g, 44%, two steps) as a white solid. ¹H NMR (500 MHz, DMSO-*d*₆, δ): 11.48 (br s, 1H), 9.48 (br s, 1H), 7.36 (s, 4H), 5.30 (s, 1H), 4.08 (s, 2H). ¹³C NMR (125 MHz, DMSO-*d*₆, δ): 161.3, 139.3, 135.0, 130.5, 129.8, 128.8, 89.6, 27.7. HRMS (*m/z*): [M + H]⁺ calcd for C₁₀H₉Cl¹⁵N₂OS, 243.0142; found 243.0192.

5-(4-Chlorophenylsulfinyl)-1H-pyrazol-3(2H)-one (4). Compound **20** was obtained from 4-chlorothiophenol and ethyl 4-chloroacetoacetate and used directly after flash column chromatography as described above. Compound **20** (1.27 g, 4.66 mmol) was mixed with *tert*-butyl hydrogen peroxide (70 wt % in water, 1.1 mL, 7.69 mmol) in CH₂Cl₂ (50 mL) at room temperature, and vanadyl acetylacetonate (0.1% mol) was added slowly. Additional *tert*-butyl hydrogen peroxide (0.5 mL, 3.50 mmol) was added to the reaction mixture after 2 h. The resulting suspension was stirred overnight at room temperature. The reaction mixture was then concentrated under vacuum and purified by flash column chromatography (ethyl acetate/hexanes = 1/4) to afford compound **23** (0.98 g) as a light yellow solid, which was not very stable. A proton NMR spectrum was taken immediately after the flash column purification. ¹H NMR (500 MHz, CDCl₃, δ): 7.46–7.34 (m, 4H), 4.20 (q, *J* = 7.5 Hz, 2H), 4.13 (s, 2H), 3.80 (s, 2H), 1.28 (t, *J* = 7.5 Hz, 3H). Therefore, **23** was used directly in the next step immediately after the flash column chromatography purification. Compound **23** (0.50 g, 1.73 mmol) was stirred in EtOH (6 mL), and an ethanolic solution of NH₂NH₂ (2 N, 0.87 mL, 1.74 mmol) was added. The resulting solution was stirred overnight at room temperature, during which time a precipitate formed. The precipitate was filtered, washed with cold EtOH, and dried in vacuo to afford **4** (0.10 g, 17%, three steps) as a white solid. ¹H NMR (500 MHz, DMSO-*d*₆, δ): 11.49 (br s, 1H), 9.75 (br s, 1H), 7.62 (d, *J* = 8.0 Hz, 2H), 7.54 (d, *J* = 9.0 Hz, 2H), 5.17 (s, 1H), 4.13–3.99 (m, 2H). ¹³C NMR (125 MHz, DMSO-*d*₆, δ): 160.9, 142.5, 135.7, 132.1, 129.1, 126.3, 90.2, 53.3. HRMS (*m/z*): [M + H]⁺ calcd for C₁₀H₉ClN₂O₂S, 256.00733; found 256.00732.

5-(4-Chloro-2,5-dimethylphenylsulfinyl)-1H-pyrazol-3(2H)-one (5). Analogous to **4**, compound **22** was prepared from 4-chloro-2,5-dimethylbenzenethiol (9 g, 52.1 mmol) to afford **22** (13.11 g). Immediately after flash chromatography, **22** (4.69 g, 14.2 mmol) was converted to **24** (3.20 g). Immediately after flash column chromatography, **24** (1.39 g, 4.00 mmol) was converted to **5** as a white solid (0.42 g, 19%, three steps). ¹H NMR (500 MHz, DMSO-*d*₆, δ): 11.52 (br s, 1H), 9.50 (br s, 1H), 7.58 (s, 1H), 7.37 (s, 1H), 5.22 (s, 1H), 4.03–3.93 (m, 2H), 2.35 (s, 3H), 2.15 (s, 3H). ¹³C NMR (125 MHz, DMSO-*d*₆, δ): 161.1, 140.8, 135.7, 134.7, 134.1, 132.5, 130.3, 126.1, 90.9, 52.3, 19.3, 16.8.

5-(4-Chlorophenylsulfonyl)-1H-pyrazol-3(2H)-one (6). Compound **20** was obtained from 4-chlorothiophenol and ethyl 4-chloroacetoacetate and used directly after flash column as described

above. Compound **20** (3.0 g, 11.0 mmol) was mixed with *tert*-butyl hydrogen peroxide (70 wt % in water, 1.5 mL, 10.5 mmol) in CH₂Cl₂ (50 mL) at room temperature, and vanadyl acetylacetonate (0.1% mol) was added slowly. Additional *tert*-butyl hydrogen peroxide (6 mL, 41.94 mmol) was added to the reaction mixture gradually until all starting material was consumed, as determined by TLC. The resulting suspension was stirred overnight at room temperature. The reaction mixture was then concentrated under vacuum and purified by flash column chromatography (ethyl acetate/hexanes = 1/4) to afford **25** (1.61 g) as a light yellow oil, which was not very stable. Therefore, **25** was used directly in the next step immediately after flash column chromatography purification. Compound **25** (1.60 g, 5.25 mmol) was stirred in EtOH (6 mL), and an ethanolic solution of NH₂NH₂ (2 N, 2.64 mL, 5.28 mmol) was added. The resulting solution was stirred overnight at room temperature, during which time a precipitate formed. The precipitate was filtered, washed with cold EtOH, and dried under vacuum to afford **6** (0.46 g, 12%, three steps) as a white solid. ¹H NMR (500 MHz, DMSO-*d*₆, δ): 11.24 (br s, 1H), 7.75 (d, *J* = 9.0 Hz, 2H), 7.67 (d, *J* = 8.5 Hz, 2H), 5.21 (s, 1H), 4.56 (s, 2H). ¹³C NMR (125 MHz, DMSO-*d*₆, δ): 159.1, 139.0, 137.2, 130.1, 129.4, 89.9, 54.1. HRMS (*m/z*): [M + H]⁺ calcd for C₁₀H₉ClN₂O₃S, 272.00224; found 272.00164.

5-(3,5-Dichlorophenylsulfonyl)-1H-pyrazol-3(2H)-one (7). Analogous to **6**, compound **21** (4.20 g) was prepared from 3,5-dichlorobenzene-1-thiol (2.5 g, 14.0 mmol). Immediately after flash chromatography, **21** (4.10 g, 13.3 mmol) was converted to **26** (2.24 g). Immediately after flash chromatography, **26** (2.14 g, 6.31 mmol) was converted to **7** as a white solid (0.38 g, 10%, three steps). ¹H NMR (500 MHz, DMSO-*d*₆, δ): 11.62 (br s, 1H), 9.55 (br s, 1H), 7.77–7.36 (m, 3H), 5.26 (s, 1H), 4.70 (s, 2H). ¹³C NMR (125 MHz, DMSO-*d*₆, δ): 161.3, 141.2, 135.0, 133.8, 129.5, 126.7, 92.1, 52.5. HRMS (*m/z*): [M + H]⁺ calcd for C₁₀H₈Cl₂N₂O₃S, 301.0408; found 301.0415.

5-(4-Chloro-2,5-dimethylphenylsulfonyl)-1H-pyrazol-3(2H)-one (8). Compound **22** was obtained from 4-chloro-2,5-dimethylbenzenethiol and ethyl 4-chloroacetoacetate and used directly after flash column chromatography as described above. Compound **22** (4.68 g, 14.1 mmol) was mixed with AcOH (5 mL) in EtOAc (10 mL), and H₂O₂ (30% in water, 10 mL, 84.6 mmol) was added. The resulting solution was left stirring at room temperature overnight after which additional H₂O₂ (30% in water, 5 mL, 42.3 mmol) was added. The reaction mixture was then evaporated under vacuum and purified by flash column chromatography (ethyl acetate/hexanes = 1/3) to afford **27** (4.34 g) as a yellowish oil, which was not very stable. Therefore, **27** was used directly in the next step immediately after flash column chromatography purification. Compound **27** (4.33 g, 11.9 mmol) was stirred in EtOH (20 mL), and an ethanolic solution of NH₂NH₂ (2 N, 5.98 mL, 11.9 mmol) was added. The resulting solution was stirred overnight at room temperature, during which time a precipitate formed. The precipitate was filtered, washed with cold EtOH, and dried under vacuum to afford **8** (0.71 g, 17%, three steps) as a white solid. ¹H NMR (500 MHz, DMSO-*d*₆, δ): 11.62 (br s, 1H), 9.59 (br s, 1H), 7.67 (s, 1H), 7.54 (s, 1H), 5.24 (s, 1H), 4.49 (s, 2H), 2.47 (s, 3H), 2.33 (s, 3H). ¹³C NMR (125 MHz, DMSO-*d*₆, δ): 160.3, 138.8, 137.7, 135.2, 133.9, 132.5, 132.4, 131.0, 91.8, 53.1, 43.3, 19.1. HRMS (*m/z*): [M + H]⁺ calcd for C₁₂H₁₃ClN₂O₃S, 306.9705; found 306.9713.

Synthesis of Ether Analogues (9–13) via Method A. 5-((4-Chlorophenoxy)methyl)-1H-pyrazol-3(2H)-one (9). A solution of 4-chlorophenol (6.4 g, 50 mmol) in THF (25 mL) was treated with NaH (60% in mineral oil, 2 g, 50 mmol) at 0 °C. In another flask, a solution of ethyl 4-chloroacetoacetate (10.21 mL, 75 mmol) in THF (25 mL) was treated with NaH (60% in mineral oil, 3.5 g, 75 mmol) at –20 °C. The resulting yellowish suspension was slowly added to the solution of sodium 4-chlorophenoxide, which was kept at 0 °C. After the addition of DMF (10 mL), the reaction temperature was slowly raised to 70 °C. After the reaction mixture was stirred at 70 °C overnight, it was cooled and evaporated to dryness. The residue was purified by flash column chromatography (ethyl acetate/hexanes = 1/9) to afford **28** (10.7 g, contains 30% 4-chloroacetonacetate) as a

yellowish oil. The obtained mixture was used directly in the next step. To the mixture of **28** and 4-chlorophenol (10.7 g, assumed 41.7 mmol) was added an ethanolic solution of NH₂NH₂ (2 N, 14.5 mL, 29.0 mmol). The resulting solution was stirred overnight at room temperature, during which time a precipitate formed. The precipitate was filtered, washed with cold EtOH, and dried under vacuum to afford **9** (1.38 g, 13%, two steps) as a white solid. ¹H NMR (500 MHz, DMSO-*d*₆, δ): 11.79 (br s, 1H), 9.56 (br s, 1H), 7.33 (d, *J* = 9.0 Hz, 2H), 7.02 (d, *J* = 9.0 Hz, 2H), 5.52 (s, 1H), 4.92 (s, 2H). ¹³C NMR (125 MHz, DMSO-*d*₆, δ): 160.2, 157.0, 139.2, 129.3, 124.6, 116.6, 89.5, 62.1.

5-((4-Ethylphenoxy)methyl)-1H-pyrazol-3(2H)-one (10). Analogous to **9**, compound **29** was prepared from 4-ethylphenol (3.0 g, 24.6 mmol). The mixture of **29** and 4-ethylphenol (4.05 g, assumed 16.2 mmol) was converted to **10** (1.62 g, 30%, two steps) as a white solid. ¹H NMR (500 MHz, DMSO-*d*₆, δ): 11.75 (br s, 1H), 9.50 (br s, 1H), 7.10 (d, *J* = 8.0 Hz, 2H), 6.89 (d, *J* = 8.5 Hz, 2H), 5.50 (s, 1H), 4.87 (s, 2H), 2.54–2.51 (m, 2H), 1.13 (t, *J* = 7.5 Hz, 3H). ¹³C NMR (125 MHz, DMSO-*d*₆, δ): 160.0, 156.2, 140.3, 136.1, 128.7, 114.6, 89.4, 61.6, 27.4, 16.0.

5-((3-Ethylphenoxy)methyl)-1H-pyrazol-3(2H)-one (11). Analogous to **9**, compound **30** was prepared via method A from 3-ethylphenol (3.0 g, 24.6 mmol). The mixture of **30** and 3-ethylphenol (1.81 g, assumed 7.23 mmol) was converted to **10** (0.30 g, 6%, two steps) as a white solid. ¹H NMR (500 MHz, DMSO-*d*₆, δ): 11.79 (br s, 1H), 9.55 (br s, 1H), 7.18 (t, *J* = 7.8 Hz, 1H), 6.83–6.79 (m, 3H), 5.52 (s, 1H), 4.89 (s, 2H), 2.56 (q, *J* = 7.5 Hz, 2H), 1.16 (t, *J* = 7.5 Hz, 3H). ¹³C NMR (125 MHz, DMSO-*d*₆, δ): 160.7, 158.2, 145.4, 139.3, 129.3, 120.4, 114.3, 111.8, 89.8, 61.0, 28.3, 15.6.

5-((3-*tert*-Butylphenoxy)methyl)-1H-pyrazol-3(2H)-one (12). Analogous to **9**, compound **31** was prepared via method A from 3-*tert*-butylphenol (3.0 g, 20.0 mmol). The mixture of **31** and 3-*tert*-butylphenol (2.47 g, assumed 8.86 mmol) was treated with NH₂NH₂ (2 N, 4.40 mL, 8.80 mmol) to give **10** (1.52 g, 10%, two steps) as a white solid. ¹H NMR (500 MHz, DMSO-*d*₆, δ): 11.72 (br s, 1H), 9.50 (br s, 1H), 7.20 (t, *J* = 8.0 Hz, 1H), 6.97–6.80 (m, 3H), 5.52 (s, 1H), 4.91 (s, 2H). ¹³C NMR (125 MHz, DMSO-*d*₆, δ): 160.7, 157.9, 152.4, 138.7, 129.0, 117.8, 112.3, 111.1, 89.7, 61.0, 34.5, 31.3.

5-((3,5-Dichlorophenoxy)methyl)-1H-pyrazol-3(2H)-one (13). Analogous to **9**, compound **32** was prepared via method A from 3,5-dichlorophenol (2.0 g, 12.3 mmol). The mixture of **32** and 3,5-dichlorophenol (1.10 g, assumed 3.78 mmol) was treated with NH₂NH₂ (2 N, 1.90 mL, 3.80 mmol) to give **13** (66.1 mg, 2%, two steps) as a white solid. See below (method B) for characterization of **13**.

5-((3,5-Bis(trifluoromethyl)phenoxy)methyl)-1H-pyrazol-3(2H)-one (14). Analogous to **9**, compound **33** was prepared via method A from 3,5-bis(trifluoromethyl)phenol (1.00 mL, 5.93 mmol). The mixture of **33** and 3,5-bis(trifluoromethyl)phenol (0.72 g, assumed 2.00 mmol) was treated with NH₂NH₂ (2 N, 1.00 mL, 2.00 mmol) to give **14** (0.40 g, 20%, two steps) as a white solid. ¹H NMR (500 MHz, DMSO-*d*₆, δ): 11.62 (br s, 1H), 9.50 (br s, 1H), 7.99 (s, 2H), 7.86 (s, 1H), 5.35 (s, 1H), 4.31 (s, 2H). ¹³C NMR (125 MHz, DMSO-*d*₆, δ): 159.8, 140.9, 131.2, 130.9, 130.5, 130.2, 127.6, 127.2, 124.5, 121.8, 119.1, 118.8, 89.0, 27.6.

Synthesis of Ether Analogues (13, 15–19) via Method B. Detailed experimental procedures and characterization of **35**, **36**, **39**, **41**, and **42–47** can be found in the Supporting Information.

5-((3,5-Dichlorophenoxy)methyl)-1H-pyrazol-3(2H)-one (13). EtOAc (3.20 mL, 32.7 mmol) was added to a solution of LiHMDS (1 N in THF, 75.0 mL, 75.0 mmol) at 0 °C and stirred. After 60 min, a THF solution of **42** (8.55 g, 32.4 mmol) was added dropwise at –78 °C. After the resulting solution was stirred at –78 °C for another 8 h, the reaction mixture was quenched with diluted HCl (0.25 N), the pH was adjusted to 3–5, and the aqueous layer was extracted with Et₂O. The combined organic layer was dried over Na₂SO₄ and concentrated under vacuum. The residue was purified by flash column chromatography (ethyl acetate/hexanes = 1/9) to give ethyl 4-(3,5-dichlorophenoxy)-3-oxobutanoate (3.28 g) as a white solid. The proton NMR spectrum was taken immediately after

recrystallization (ethyl acetate/hexanes). ^1H NMR (500 MHz, CDCl_3 , δ): 7.02 (t, $J = 1.7$ Hz, 1H), 6.81 (d, $J = 1.7$ Hz, 2H), 4.68 (s, 2H), 4.21 (q, $J = 7$ Hz, 2H), 3.61 (s, 2H), 1.28 (t, $J = 7$ Hz). Ethyl 4-(3,5-dichlorophenoxy)-3-oxobutanoate was used directly in the next step immediately after the flash column chromatography purification. Ethanolic hydrazine (2 N, 5.60 mL, 11.2 mmol) was added to a solution of ethyl 4-(3,5-dichlorophenoxy)-3-oxobutanoate (3.28 g, 11.3 mmol) in EtOH (25 mL). The resulting solution was stirred at room temperature overnight. The reaction mixture was then evaporated under vacuum, purified by flash column chromatography (ethyl acetate/hexanes = 1/2), and recrystallized in ethyl acetate/hexanes to give **13** (0.88 g, 11%, two steps) as white crystals. ^1H NMR (500 MHz, $\text{DMSO}-d_6$, δ): 11.82 (br s, 1H), 9.54 (br s, 1H), 7.16 (s, 1H), 7.12 (d, $J = 1.5$ Hz, 2H), 5.53 (s, 1H), 4.99 (s, 2H). ^{13}C NMR (125 MHz, $\text{DMSO}-d_6$, δ): 161.0, 159.4, 137.8, 134.6, 120.6, 114.2, 90.7, 61.5. Anal. Calcd for $\text{C}_{10}\text{H}_8\text{Cl}_2\text{N}_2\text{O}_2$: C, 46.36; H, 3.11; Cl, 27.37; N, 10.81. Found: C, 46.40; H, 3.08; Cl, 27.24; N, 10.65. All values are given as percentages.

5-((3,5-Difluorophenoxy)methyl)-1H-pyrazol-3(2H)-one (15). Analogous to **13**, compound **15** was prepared via method B from **43** (1.24 g, 5.36 mmol) to afford initially ethyl 4-(3,5-difluorophenoxy)-3-oxobutanoate (0.89 g, 3.44 mmol). Because of instability, immediately after flash column chromatography, ethyl 4-(3,5-difluorophenoxy)-3-oxobutanoate (0.89 g, 3.44 mmol) was treated with NH_2NH_2 (2 N in EtOH, 1.70 mL, 3.40 mmol) to give **15** as a white solid (50.9 mg, 5%, two steps). ^1H NMR (500 MHz, $\text{DMSO}-d_6$, δ): 11.82 (br s, 1H), 9.53 (br s, 1H), 6.80–6.79 (m, 3H), 5.56 (s, 1H), 4.95 (s, 2H). ^{13}C NMR (125 MHz, $\text{DMSO}-d_6$, δ): 0.1, 164.0, 162.1, 162.0, 160.0, 146.4, 137.8, 99.1, 98.9, 96.4, 90.7, 61.8.

5-((3,5-Dibromophenoxy)methyl)-1H-pyrazol-3(2H)-one (16). Analogous to **13**, compound **16** was prepared via method B from **44** (1.07 g, 3.03 mmol) to afford initially ethyl 4-(3,5-dibromophenoxy)-3-oxobutanoate (0.35 g). Immediately after flash column, ethyl 4-(3,5-dibromophenoxy)-3-oxobutanoate (0.35 g, 0.92 mmol) was treated with NH_2NH_2 (2 N in EtOH, 0.46 mL, 0.92 mmol) to give **16** as a white solid (23.7 mg, 2%, two steps). ^1H NMR (500 MHz, $\text{DMSO}-d_6$, δ): 11.80 (br s, 1H), 9.52 (br s, 1H), 7.39 (s, 1H), 7.28 (m, 2H), 5.55 (s, 1H), 4.99 (s, 1H). ^{13}C NMR (125 MHz, $\text{DMSO}-d_6$, δ): 161.0, 159.5, 137.7, 125.9, 122.8, 117.4, 90.6, 61.5.

5-((3-Bromophenoxy)methyl)-1H-pyrazol-3(2H)-one (17). Analogous to **13**, compound **17** was prepared via method B from **45** (2.43 g, 8.87 mmol) to afford initially ethyl 4-(3-bromophenoxy)-3-oxobutanoate (1.07 g). Immediately after flash column, ethyl 4-(3-bromophenoxy)-3-oxobutanoate (1.07 g, 3.55 mmol) was treated with NH_2NH_2 (2 N in EtOH, 1.70 mL, 3.40 mmol) to give **17** as a white solid (0.42 g, 18%, two steps). ^1H NMR (500 MHz, $\text{DMSO}-d_6$, δ): 11.78 (br s, 1H), 9.50 (br s, 1H), 7.26–7.23 (m, 1H), 7.14–7.13 (m, 1H), 7.02–7.00 (m, 2H), 5.58 (s, 1H), 4.96 (s, 2H). ^{13}C NMR (125 MHz, $\text{DMSO}-d_6$, δ): 161.6, 159.1, 138.4, 131.2, 123.8, 122.1, 117.6, 114.3, 90.5, 61.3.

5-((Biphenyl-3-yloxy)methyl)-1H-pyrazol-3(2H)-one (18). Analogous to **13**, compound **18** was prepared via method B from **46** (0.74 g, 2.74 mmol) to afford initially ethyl 4-(biphenyl-3-yloxy)-3-oxobutanoate (0.50 g). Immediately after flash column, ethyl 4-(biphenyl-3-yloxy)-3-oxobutanoate (0.50 g, 1.68 mmol) was treated with NH_2NH_2 (2 N in EtOH, 0.84 mL, 1.68 mmol) to give **18** as a white solid (0.19 g, 27%, two steps). ^1H NMR (500 MHz, $\text{DMSO}-d_6$, δ): 11.80 (br s, 1H), 9.50 (br s, 1H), 7.67–6.99 (m, 9H), 5.55 (s, 1H), 5.02 (s, 2H). ^{13}C NMR (125 MHz, $\text{DMSO}-d_6$, δ): 161.3, 158.6, 138.7, 141.7, 140.0, 130.0, 128.9, 127.7, 126.8, 119.4, 113.9, 113.0, 90.3, 60.8.

5-((5-Phenylbiphenyl-3-yloxy)methyl)-1H-pyrazol-3(2H)-one (19). Analogous to **13**, compound **19** was prepared via method B from **47** (0.61 g, 1.75 mmol) to afford initially ethyl 4-(5-phenylbiphenyl-3-yloxy)-3-oxobutanoate (0.45 g). Immediately after flash column, ethyl 4-(5-phenylbiphenyl-3-yloxy)-3-oxobutanoate (0.45 g, 1.21 mmol) was treated with NH_2NH_2 (2 N in EtOH, 0.60 mL, 1.20 mmol) to give **19** as a white solid (0.19 g, 27%, two steps). ^1H NMR (500 MHz, $\text{DMSO}-d_6$, δ): 11.82 (br s, 1H), 9.50 (br s, 1H), 7.76 (d, $J = 8.0$ Hz, 4H), 7.50–7.38 (m, 7H), 7.27 (s, 2H), 5.60 (s, 1H), 5.13 (s, 2H). ^{13}C NMR

(125 MHz, $\text{DMSO}-d_6$, δ): 161.3, 159.1, 142.3, 140.0, 139.0, 129.0, 127.8, 127.0, 118.0, 112.3, 90.4, 61.2.

In Vitro Microsomal Stability of Compound 1 and Minaprine. General Methods, Reagents, and Materials. The microsome assay was measured on a Beckman HPLC system using Luna C18 (2) column (4.6 mm \times 150 mm, 5 μm ; Phenomenex, Torrance, CA) at a flow rate of 1 mL/min at 254 nm for minaprine and 260 nm for **1**. Solid phase extraction was carried out using Waters Sep-PakVac C18 1 cc cartridges (Waters Chromatography, Milford, MA). NADPH regeneration solutions and rat liver microsomes were purchased from Bectin-Dickinson.

To PBS (10 mL) was added NADPH regeneration buffer A (500 μL) and NADPH regeneration buffer B (100 μL) to make the PBS+ solution. To the PBS+ solution (255 μL) was added the compound of interest (30 μL of 150 μM stock in PBS+) in an Eppendorf tube. Each reaction mixture was carried out in PBS (pH 7.4), which contained 1 mg/mL microsomal protein with 1.3 mM NADP^+ , 3.3 mM glucose 6-phosphate, 0.4 U/mL glucose 6-phosphate dehydrogenase, and 3.3 mM magnesium chloride. The tubes were vortexed and equilibrated at 37 $^\circ\text{C}$. The samples were incubated at 37 $^\circ\text{C}$ for 0 and 20 min after the rat liver microsomes (15 μM) were added. Acetonitrile (40 μL) and haloperidol (internal standard, 100 μL) were added as a quench solution. The reaction mixture was vortexed and left in a -78 $^\circ\text{C}$ ice bath immediately after it was quenched. The samples were centrifuged (13.4 krpm, 12 min), and the supernatant was loaded onto a Waters Sep-PakVac C18 1 cc SPE cartridge. The loaded SPE column was washed with H_2O (2 \times 1 mL), and the compounds were eluted with acetonitrile/ H_2O = 1/1 (2 \times 1 mL). The solvent was removed under vacuum. The samples were reconstituted in $\text{DMSO}/\text{H}_2\text{O}$ = 1/9 (25 μL), and an aliquot (20 μL) was analyzed by HPLC (isocratic, acetonitrile/ H_2O = 25/75, 60 min, 0.1% TFA). The response ratio (RR) was calculated by dividing the peak area of the analyte by the peak area of the internal standard. Peak integrals were normalized by dividing by the area for the peak at $t = 0$ min. Sample HPLC spectrum and RR data can be found in the Supporting Information.

Metabolite Profiling of Compound 1. Compound **1** was incubated with rat liver microsomes and NADPH regeneration buffers as described above for the in vitro microsomal stability study of **1**. To the PBS+ solution (85 μL) was added **1** (10 μL of 150 μM stock in PBS+). The sample was incubated at 37 $^\circ\text{C}$ for 0, 5, 10, 20, 40, and 60 min after the rat liver microsomes (15 μM) were added. Acetonitrile (50 μL) was added as a stop solution. The mixture was vortexed and left on a -78 $^\circ\text{C}$ ice bath immediately after it was quenched. The samples were centrifuged (13.4 krpm, 12 min), and the supernatant (20 μL) was directly analyzed by HPLC (isocratic, acetonitrile/ H_2O = 25/75, 30 min, 0.1% TFA). Compounds **4** (20 μL , 10 μM) and **6** (20 μL , 10 μM) were analyzed by the same HPLC program. Spectra of the microsomal incubation residue of **1**, standard solution of **4**, and standard solution of **6** were compared in parallel.

Further Metabolite Profiling of 1 and 3. Metabolite studies were also performed at Aprelica, Inc. (Watertown, MA). Samples were analyzed by LC/MS/MS using either an Agilent 6410 mass spectrometer coupled with an Agilent 1200 HPLC instrument and a CTC PAL chilled autosampler or an ABI2000 mass spectrometer coupled with an Agilent 1100 HPLC instrument and a CTC PAL chilled autosampler. After separation of compounds on a C18 reverse phase HPLC column using an acetonitrile–water gradient system, peaks were analyzed by mass spectrometry using ESI ionization in MRM mode.

Each test agent (**1** and **3**) was incubated in duplicate at 5 μM with or without rat liver microsomes in the presence and absence of NADPH. After 0, 10, 20, 40, and 60 min of incubation, an aliquot was removed from each reaction and the protein was precipitated with acetonitrile containing internal standard. The supernatant was analyzed by LC/MS/MS. Detailed experimental data and HPLC and MS spectra can be found in the Supporting Information.

Mutant SOD1-Induced Cytotoxicity Protection Assay. Viability and EC_{50} values of **1**–**19** were determined according to the previously reported assay procedure.²⁰ PC12 cells expressing mutant G93A SOD1 were seeded at 15 000 cells/well in 96-well plates and

incubated for 24 h prior to compound addition. Compounds were assayed in 12-point dose–response experiments to determine potency and efficacy. The highest compound concentration tested was 32 μM , which was decreased by one-half with each subsequent dose. After 24 h of incubation with the compounds, MG132 was added at a final concentration of 100 nM. MG132 is a well-characterized proteasome inhibitor, which enhances the appearance of protein aggregation by blocking the proteosomal clearance of aggregated proteins. Cell viability was measured 48 h later using a fluorescent viability probe, Calcein-AM (Molecular Probes). Briefly, cells were washed twice with PBS, Calcein-AM was added at a final concentration of 1 μM for 20 min at room temperature, and fluorescence intensity was read in a POLARstar fluorescence plate reader (BMG). Fluorescence data were coupled with compound structural data, then stored and analyzed using the CambridgeSoft Chemoffice Enterprise Ultra software package.

In Vitro ADME Assays. In vitro microsomal stability of 7 and 9, aqueous solubility, and Caco-2 permeability of 7, 9, and 13 were determined according to the previously reported procedure.²¹ In vitro microsomal stability of 13 was obtained from Biogen Idec.

Preliminary Cortical Neuron Permeability. Primary rat cortical tissue was purchased from Neuromics Inc., Edina, MN, and used to initiate primary cortical neuron cultures. The tissue was isolated from microsurgically dissected E18 embryonic Sprague–Dawley or Fischer 344 rat brain and shipped in a nutrient rich medium under refrigeration.

To isolate neurons, the tissue was incubated with papain at 2 mg/mL in Hibernate without calcium for 30 min at 37 °C. The enzymatic solution was then removed and 1 mL of culture medium (Neurobasal, B27, 0.5 mM glutamine) was added. A sterile Pasteur pipet was used to gently disperse the cells, which were then washed, resuspended, and counted. The cells were plated on poly-D-lysine coated 96-well plates at a density of 20 000 cells/well and incubated at 37 °C in a 5% CO₂-humidified atmosphere for 5 days prior to use in compound testing. By microscopic inspection, the resulting culture consisted of ~90% neurons.

Test compounds were assayed in six-point dose response experiments. The highest compound concentration tested was 100 μM , which was then diluted by approximately one-third with each subsequent dose. After 24 h of incubation with the compounds, MG132 was added at a final concentration of 100 nM, a dose that produces an approximately 70% loss of viability. Cell viability was measured 48 h later using the fluorescent viability probe, Calcein-AM (Molecular Probes, Invitrogen, Carlsbad, CA). Briefly, cells were washed twice with PBS, Calcein-AM was added at a final concentration of 1 μM for 20 min at room temperature, and fluorescence intensity was then read in a POLARstar fluorescence plate reader (BMG). Compounds that restored viability at any dose to a level equal to or higher than 5 standard deviations from MG132 controls were considered active.

In Vivo Mouse Drug Steady-State Level Determination and in Vivo Brain Penetration. See Supporting Information.

In Vivo PK Profiling. In vivo PK profiling was performed by administering a 300 mg/kg bolus intraperitoneal injection of 13 into B6SJL mice. Blood and brain samples were collected at 0, 1, 3, 6, 12, and 24 h time points and flash frozen in liquid nitrogen, stored at –80 °C, and shipped to Aprelica, Inc. for analysis. The analysis was carried out as for in vivo mouse drug steady-state level determination and in vivo brain penetration described in Supporting Information.

Effect of Compound 13 on Potassium Channels. FASTPatch hERG screen assay, using cloned hERG potassium channels expressed in human embryonic kidney cells (HEK293), was carried out by ChanTest Corporation (Cleveland, OH).

In Vivo SOD1 G93A ALS Mice Study of 13. G93A SOD1 mice and littermate SOD1 mice were mated with B6SJL females, and the offspring were genotyped by PCR using tails. A 12 h light–dark cycle was maintained, and animals were given free access to food and water. Control and transgenic mice of the same age (± 3 days) and from the same “F” generation were selected from multiple litters to form experimental cohorts ($n = 20$ per group). Standardized criteria for age,

weight, and parentage were used for placing individual mice into experimental groups/cohorts. Wild type mice were used for initial toxicity, tolerability, and pharmacokinetics studies. The tolerable dose range and LD₅₀ for 13 was determined in the wild type mice by increasing the dose b.i.d. 1-fold each injection and observed at 75 mg/kg. Drug steady-state level was determined in animals that had been dosed for 1 week prior to sacrifice. The dosing levels of 1.0, 10, and 20 mg/kg once a day were administered throughout the levels of the G93A mice.

Efficacy was measured using end points that clearly indicate neuroprotective function. These include amelioration of degenerative changes in the spinal cord, improved motor function, and prolonged survival. The mice cohorts were sacrificed at end stage disease using criteria for euthanasia, followed temporally for survival analyses. Mice were observed three times daily (morning, noon, and later afternoon) throughout the experiment. Mice were euthanized when disease progression was sufficiently severe that they were unable to initiate movement and right themselves after gentle prodding for 30 s.

Data sets were generated and analyzed for each clinical and neuropathological measure. Effects on behavior and neuropathology were compared in treatment and control groups. Dose-dependent effects were assessed in each treatment group using multiple two-sided ANOVA tests. Multiple comparisons in the same subject groups were dealt with post hoc. Kaplan–Meier analysis was used for survival function. All other statistical analyses were performed using Student's *t* test. Data are expressed as the mean \pm SEM. Statistical comparisons of histological data were made by ANOVA.

■ ASSOCIATED CONTENT

📄 Supporting Information

Experimental details and data for 35, 36, 39, 41, and 42–47; HPLC data and spectra for 1–19; HPLC spectra and data of microsomal stability of minaprine and 1; data and spectra of metabolite profiling of 1 and 3; bioanalysis data of in vivo mouse steady-state level study and in vivo blood–brain barrier study of 13; data for the effect of 13 on hERG potassium channel; data for the effect of 13 on enzymes and receptors. This material is available free of charge via the Internet at <http://pubs.acs.org>.

■ AUTHOR INFORMATION

Corresponding Author

*Address: Department of Chemistry, Northwestern University, 2145 Sheridan Road, Evanston, IL 60208-3113. Phone: 1-847-491-5653. Fax: 1-847-491-7713. E-mail: Agman@chem.northwestern.edu.

■ ACKNOWLEDGMENTS

We thank the National Institutes of Health (Grant 1R43NS057849), the ALS Association (TREAT program), the Department of Defense (Grant AL093052), and the Center for ALS Research at the University of Pittsburgh, PA, for their generous support of the research project. The authors are grateful to Biogen Idec Inc. for carrying out the in vivo rat PK profiling tests, in vitro P450 reversible inhibition study, the plasma binding affinity assay, and the hERG inhibition assays; and MDS Pharma Service (now Ricerca Biosciences, LLC) for carrying out the LeadProfilingScreen of 13.

■ ABBREVIATIONS USED

ADME, absorption, distribution, metabolism, and excretion; ALS, amyotrophic lateral sclerosis; ASP, arylsulfanyl pyrazolone; CYP, cytochrome P450; FALS, familial amyotrophic lateral sclerosis; HEK, human embryonic kidney; hERG, human ether-a-go-go-related gene; HTS, high-throughput screening;

MRM, multiple reaction monitoring; PK, pharmacokinetics; SOD1, Cu/Zn superoxide dismutase 1; SALS, sporadic amyotrophic lateral sclerosis

REFERENCES

- (1) Bruijn, L. I.; Miller, T. M.; Cleveland, D. W. Unraveling the mechanisms involved in motor neuron degeneration in ALS. *Annu. Rev. Neurosci.* **2004**, *27*, 723–749.
- (2) Hirtz, D.; Thurman, D. J.; Gwinn-Hardy, K.; Mohamed, M.; Chaudhuri, A. R.; Zalutsky, R. How common are the “common” neurologic disorders? *Neurology* **2007**, *68*, 326–337.
- (3) Cronin, S.; Hardiman, O.; Traynor, B. J. Ethnic variation in the incidence of ALS. *Neurology* **2007**, *68*, 1002–1007.
- (4) Haley, R. W. Excess incidence of ALS in young Gulf War veterans. *Neurology* **2003**, *61*, 750–756.
- (5) Horner, R. D.; Kamins, K. G.; Feussner, J. R.; Grambow, S. C.; Hoff-Lindquist, J.; Harati, Y.; Mitumoto, H.; Pascuzzi, R.; Spencer, P. S.; Tim, R.; Howard, D.; Smith, T. C.; Ryan, M. A. K.; Coffman, C. J.; Kasarskis, E. J. Occurrence of amyotrophic lateral sclerosis among Gulf War veterans. *Neurology* **2003**, *61*, 742–749.
- (6) Weisskopf, M. G.; O'Reilly, E. J.; McCullough, M. L.; Calle, E. E.; Thun, M. J.; Cudkovic, M.; Ascherio, A. Prospective study of military service and mortality from ALS. *Neurology* **2005**, *64*, 32–37.
- (7) Rowland, L. P.; Shneider, N. A. Amyotrophic lateral sclerosis. *N. Engl. J. Med.* **2001**, *344*, 1688–1700.
- (8) Miller, R. G.; Mitchell, J. D.; Moore, D. H. Riluzole for amyotrophic lateral sclerosis (ALS)/motor neuron disease (MND). *Amyotrophic Lateral Scler. Other Mot. Neuron Disord.* **2003**, *4*, 191–206.
- (9) Rosen, D. R.; Siddique, T.; Patterson, D.; Figlewicz, D. A.; Sapp, P.; Hentati, A.; Donaldson, D.; Goto, J.; O'Regan, J. P.; Deng, H.; Rahmani, Z.; Krizus, A.; McKenna-Yasek, D.; Cayabyab, A.; Gaston, S. M.; Berger, R.; Tanzi, R. E.; Halperin, J. J.; Herzfeldt, B.; Van den Bergh, R.; Hung, W.; Bird, T.; Deng, G.; Mulder, D. W.; Smyth, C.; Laing, N. G.; Soriano, E.; Pericak-Vance, M. A.; Haines, J.; Rouleau, G. A.; Gusella, J.; Horvitz, H. R.; Brown, R. H. Jr. Mutations in Cu/Zn superoxide dismutase gene are associated with familial amyotrophic lateral sclerosis. *Nature* **1993**, *362*, 59–62.
- (10) Pasinelli, P.; Brown, R. H. Molecular biology of amyotrophic lateral sclerosis: insight from genetics. *Nat. Rev. Neurosci.* **2006**, *7*, 710–723.
- (11) Mulder, D. W.; Kurland, L. T.; Offord, K. P.; Beard, C. M. Familial adult motor neuron disease: amyotrophic lateral sclerosis. *Neurology* **1986**, *36*, 511–517.
- (12) Pramatarova, A.; Figlewicz, D. A.; Krizus, A.; Han, F. Y.; Ceballos-Picot, I.; Nicole, A.; Dib, M.; Meininger, V.; Brown, R. H.; Rouleau, G. A. Identification of new mutations in the Cu/Zn superoxide dismutase gene of patients with familial amyotrophic lateral sclerosis. *Am. J. Hum. Genet.* **1995**, *56*, 592–596.
- (13) Ryu, H.; Ferrante, R. J. Translational therapeutic strategies in amyotrophic lateral sclerosis. *Mini-Rev. Med. Chem.* **2007**, *7*, 141–150.
- (14) Andersen, P. M.; Sims, K. B.; Xin, W. W.; Kiely, R.; O'Neill, G.; Ravits, J.; Piro, E.; Harati, Y.; Brower, R. D.; Levine, J. S.; Heinicke, H. U.; Seltzer, W.; Boss, M.; Brown, R. H. Jr. Sixteen novel mutations in the Cu/Zn superoxide dismutase gene in amyotrophic lateral sclerosis: a decade of discoveries, defects and diputes. *Amyotrophic Lateral Scler. Other Mot. Neuron Disord.* **2003**, *4*, 62–73.
- (15) Brown, R. H. Jr.; Robberecht, W. Amyotrophic lateral sclerosis: pathogenesis. *Semin. Neurol.* **2001**, *21*, 131–139.
- (16) Newbery, H. J.; Abbott, C. M. Of mice, men and motor neurons. *Trends Mol. Med.* **2002**, *8*, 88–92.
- (17) Bruijn, L. I.; Houseweart, M. K.; Kato, S.; Anderson, K. L.; Anderson, S. D.; Ohama, E.; Reaume, A. G.; Scott, R. W.; Cleveland, D. W. Aggregation and motor neuron toxicity of an ALS-linked SOD1 mutant independent from wild-type SOD1. *Science* **1998**, *281*, 1851–1854.
- (18) Matsumoto, G.; Stojanovic, A.; Holmber, C. I.; Kim, S.; Morimoto, R. I. Structural properties and neuronal toxicity of amyotrophic lateral sclerosis-associated Cu/Zn superoxide dismutase 1 aggregates. *J. Cell Biol.* **2005**, *171*, 75–85.
- (19) Matsumoto, G.; Kim, S.; Morimoto, R. I. Huntingtin and mutant SOD1 form aggregate structures with distinct molecular properties in human cells. *J. Biol. Chem.* **2006**, *281*, 4477–4485.
- (20) Benmohamed, R.; Arvanites, A. C.; Silverman, R. B.; Morimoto, R. I.; Ferrante, R. J.; Kirsch, D. R. Identification of compounds protective against G93A SOD1 toxicity for the treatment of amyotrophic lateral sclerosis. *Amyotrophic Lateral Scler. Other Mot. Neuron Disord.* **2011**, *12*, 87–96.
- (21) Chen, T.; Benmohamed, R.; Arvanites, A. C.; Ranaivo, H. R.; Morimoto, R. I.; Ferrante, R. J.; Watterson, D. M.; Kirsch, D. R.; Silverman, R. B. Arylsulfanyl pyrazolones block mutant SOD1-G93A aggregation. Potential application for the treatment of amyotrophic lateral sclerosis. *Bioorg. Med. Chem.* **2011**, *19*, 613–622.
- (22) Basak, A.; Barlan, A. U.; Yamamoto, H. Catalytic enantioselective oxidation of sulfides and disulfides by a chiral complex of bis-hydroxamic acid and molybdenum. *Tetrahedron: Asymmetry* **2006**, *17*, 508–511.
- (23) Zhang, W.; Yamamoto, H. Vanadium-catalyzed asymmetric epoxidation of homoallylic alcohols. *J. Am. Chem. Soc.* **2007**, *129*, 286–287.
- (24) Sonda, S.; Kawahara, T.; Murozono, T.; Sato, N.; Asona, K.; Haga, K. Design and synthesis of orally active benzamide derivatives as potent serotonin 4 receptor agonist. *Bioorg. Med. Chem.* **2003**, *11*, 4225–4234.
- (25) Banfi, L.; Casicio, G.; Ghiron, C.; Guanti, G.; Manghisi, E.; Narisano, E.; Riva, R. Microbiological enantioselective synthesis of (S) and (R) 4-(p-anisoyloxy)-3-hydroxybutyrate as new chiral building blocks for the synthesis of β -lactam antibiotics. *Tetrahedron* **1994**, *50*, 11983–11994.
- (26) Hirner, S.; Panknin, O.; Edefuhr, M.; Somfai, P. Synthesis of aryl glycines by the α arylation of Weinreb amides. *Angew. Chem., Int. Ed.* **2008**, *47*, 1907–1909.
- (27) Gu, R.; Hameurlaine, A.; Dehaen, W. Facile one-pot synthesis of 6-monosubstituted and 6,12-disubstituted 5,11-dihydroindolo[3,2-b]carbazoles and preparation of various functionalized derivatives. *J. Org. Chem.* **2007**, *72*, 7207–7213.
- (28) Doherty, E. M.; Fotsch, M.; Bo, Y.; Chakrabarti, P. P.; Chen, N.; Gavva, N.; Han, N.; Kelly, M. G.; Kincaid, J.; Klionsky, L.; Liu, Q.; Ognyanov, V. I.; Tamir, R.; Wang, X.; Zhu, J.; Norman, M. H.; Treanor, J. J. S. Discovery of potent, orally available vanilloid receptor-1 antagonists. Structure–activity relationship of N-aryl cinnamides. *J. Med. Chem.* **2005**, *48*, 71–90.
- (29) Hillier, M. C.; Davidson, J. P.; Martin, S. F. Cyclopropane-derived peptidomimetics. design, synthesis, and evaluation of novel ras farnesyltransferase inhibitors. *J. Org. Chem.* **2001**, *66*, 1657–1671.
- (30) Nakajima, T.; Wang, R.; Elovaara, E.; Gonzalez, F. J.; Gelboin, H. V.; Raunio, H.; Pelkonen, O.; Vainio, H.; Aoyama, T. Toluene metabolism by cDNA-Expressed human hepatic cytochrome P450. *Biochem. Pharmacol.* **1997**, *53*, 271–277.
- (31) McNaney, C. A.; Drexler, D. M.; Hnatyshy, S. Y.; Zvyaga, T. A.; Knipe, J. O.; Belcastro, J. V.; Sanders, M. An automated liquid chromatography–mass spectrometry process to determine metabolic stability half-life and intrinsic clearance of drug candidates by substrate depletion. *Assay Drug Dev. Technol.* **2008**, *6*, 121–129.
- (32) (a) Mitchell, S. C.; Waring, R. H. The early history of xenobiotic sulfoxidation. *Drug Metab. Rev.* **1985**, *16*, 255–284. (b) Fruetel, J.; Chang, Y.; Collins, J.; Loew, G.; Ortiz de Montellano, P. R. Thioanisole sulfoxidation by cytochrome P450cam (CYP101): experimental and calculated absolute stereochemistries. *J. Am. Chem. Soc.* **1994**, *116*, 11643–11648.
- (33) Kerns, E. H.; Di, L. *Drug-like Properties: Concepts, Structure, Design, and Methods*; Elsevier, Inc.: Amsterdam, 2008; p 291.
- (34) Zhang, W.; Benmohamed, R.; Arvanites, A. C.; Morimoto, R. I.; Ferrante, R. J.; Kirsch, D. R.; Silverman, R. B. Cyclohexane 1,3-diones and their inhibition of mutant SOD1-dependent protein aggregation and toxicity in PC12 cells. *Bioorg. Med. Chem.* [Online early access]. DOI: 10.1016/j.bmc.2011.11.039. Published Online: Nov 30, 2011.

(35) Kerns, E. H.; Di, L. *Drug-like Properties: Concepts, Structure, Design, and Methods*; Elsevier, Inc.: Amsterdam, 2008; p 378.

(36) Kerns, E. H.; Di, L. *Drug-like Properties: Concepts, Structure Design and Methods*; Elsevier, Inc.: Amsterdam, 2008; pp 288–291.

(37) Press, B.; Di Grandi, D. Permeability for intestinal absorption: Caco-2 assay and related issues. *Curr. Drug Metab.* **2008**, *9* (9), 893–900.

(38) Ilieva, H.; Polymenidou, M.; Cleveland, D. W. Non-cell autonomous toxicity in neurodegenerative disorders: ALS and beyond. *J. Cell Biol.* **2009**, *187*, 761–772.

(39) Talber, A. M.; Tranter, G. E.; Holmes, E.; Francis, P. L. Determination of drug-plasma protein binding kinetics and equilibria by chromatographic profiling: exemplification of the method using L-tryptophan and albumin. *Anal. Chem.* **2002**, *74*, 446–452.

(40) Weisiger, R. A. Dissociation from albumin: a potentially rate-limiting step in the clearance of substances by the liver. *Proc. Natl. Acad. Sci. U.S.A.* **1985**, *82*, 1563–1567.

(41) (a) Kerns, E. H.; Di, L. *Drug-like Properties: Concepts, Structure, Design, and Methods*; Elsevier, Inc.: Amsterdam, 2008; p 234. (b) Mei, H.; Korfmacher, W.; Morrison, R. Rapid in vivo oral screening in rats: reliability, acceptance criteria, and filtering efficiency. *AAPS J.* **2006**, *8*, E493–E500.

(42) (a) Bambal, R. B.; Clarke, S. E. Cytochrome P450: structure, function and application in drug discovery and development. *Eval. Drug Candidates Preclin. Dev.* **2010**, 55–107. (b) Wang, B.; Zhou, S.-F. Synthetic and natural compounds that interact with human cytochrome P450 1A2 and implications in drug development. *Curr. Med. Chem.* **2009**, *16* (31), 4066–4218.

(43) Nagai, M.; Aoki, M.; Miyoshi, I.; Kato, M.; Pasinelli, P.; Kasai, N.; Brown, R. H. Jr.; Itoyama, Y. Rats expressing human cytosolic copper-zinc superoxide dismutase transgenes with amyotrophic lateral sclerosis: associated mutations develop motor neuron disease. *J. Neurosci.* **2001**, *21*, 9246–9254.

(44) Aoki, M.; Kato, S.; Nagai, M.; Itoyama, Y. Development of a rat model of amyotrophic lateral sclerosis expressing a human SOD1 transgene. *Neuropathology* **2005**, *25*, 365–370.

(45) Gurney, M. E.; Pu, H.; Chiu, A. Y.; Dal Canto, M. C.; Polchow, C. Y.; Alexander, D. D.; Caliendo, J.; Hentati, A.; Kown, Y. W.; Deng, H. X.; Chen, W.; Zhai, P.; Sufit, R. L.; Siddique, T. Motor neuron degeneration in mice that express a human Cu, Zn superoxide dismutase mutation. *Science* **1994**, *264*, 1772–1775.

(46) Del Signore, S. J.; Amante, D. J.; Km, J.; Stack, E. C.; Goodrich, S.; Cormier, K.; Smith, K.; Cudkowicz, M. E.; Ferrante, R. J. Combined riluzole and sodium phenylbutyrate therapy in transgenic amyotrophic lateral sclerosis mice. *Amyotrophic Lateral Scler. Other Mot. Neuron Disord.* **2009**, *10*, 85–94.

(47) Gurney, M. E.; Cutting, F. B.; Zhai, P.; Doble, A.; Taylor, C. P.; Andrus, P. K.; Hall, E. D. Benefit of vitamin E, riluzole, and gabapentin in a transgenic model of familial amyotrophic lateral sclerosis. *Ann. Neurol.* **1996**, *39*, 147–157.